Optics and Lasers in Engineering 98 (2017) 118–122

Contents lists available at ScienceDirect

Optics and Lasers in Engineering

journal homepage: www.elsevier.com/locate/optlaseng

Integrated calibration of multiview phase-measuring profilometry

Yeong Beum Lee, Min H. Kim*

KAIST, 291 Daehak-ro, Yuseong-gu, Daejeon, 34141, Korea

A B S T R A C T

Phase-measuring profilometry (PMP) measures per-pixel height information of a surface with high accuracy. Height information captured by a camera in PMP relies on its screen coordinates. Therefore, a PMP measurement from a view cannot be integrated directly to other measurements from different views due to the intrinsic difference of the screen coordinates. In order to integrate multiple PMP scans, an auxiliary calibration of each camera's intrinsic and extrinsic properties is required, in addition to principal PMP calibration. This is cumbersome and often requires physical constraints in the system setup, and multiview PMP is consequently rarely practiced. In this work, we present a novel multiview PMP method that yields three-dimensional global coordinates directly so that three-dimensional measurements can be integrated easily. Our PMP calibration parameterizes intrinsic and extrinsic properties of the configuration of both a camera and a projector simultaneously. It also does not require any geometric constraints on the setup. In addition, we propose a novel calibration target that can remain static without requiring any mechanical operation while conducting multiview calibrations, whereas existing calibration methods require manually changing the target's position and orientation. Our results validate the accuracy of measurements and demonstrate the advantages on our multiview PMP.

1. Introduction

Phase measuring profilometry (PMP) has been widely used for professional applications of *highly accurate* height measurements. A projector in PMP illuminates a surface with a periodic sequence of sinusoidal patterns. A per-pixel height profile can be then driven from phase shifts of the sinusoidal patterns, captured by a camera. To obtain heights from phase shifts, PMP calibration is an essential process that defines a geometric relationship between the camera and the projector.

The traditional PMP calibration is designed to measure height per pixel from a captured image, i.e., the captured height information is valid in screen coordinates of the camera, which cannot be easily integrated to other views [1–4]. In order to integrate multiple PMP measurements, an auxiliary calibration of the camera's extrinsic properties is necessary. Xiao et al. [5] and Albers et al. [6] proposed a multiview calibration method by applying an extrinsic calibration method to determine camera properties to calculate perspective projection. These previous methods rely on the traditional Zhang method [7] to obtain the extrinsic properties of cameras. They therefore inherit the fundamental drawbacks of the Zhang method, whick requires multiple input images by mechanically changing the orientation of a checkerboard target, a process that is cumbersome and undesirable for microscale profiling systems [5,6,8–13]. Alternatively, Liu et al. [14], Zhu et al. [15], Villa et al. [16] and Gdeisat et al. [17] also introduced multiview PMP methods that can provide three-dimensional global coordinates without using the Zhang method. Instead, they still require additional calibration process with changing the target positions or orientations using an expensive hardware such as a high-precision linear Z-stage. This process is therefore cumbersome and can cause unpredicted errors when mechanically operating the target.

In this work, we propose a novel PMP calibration method to address these practical issues of additional extrinsic calibration and mechanical operations in state-of-the-art calibration approaches for achieving multiview PMP [5,6,16,17]. Different from other methods, our integrated PMP calibration process allows us to measure not only height but also (x, y) coordinates in the three-dimensional global coordinates system, allowing for direct integration of multiview PMP measurements without requiring any additional calibration of camera extrinsic parameters. In addition, our method captures only a single static scene without changing the target's orientation, which minimizes any potential errors that might occur while operating the target, while conducting calibration and scanning. Finally, our calibration does not require any constraints in the setup or any additional expensive instruments, such as a high-precision Z-stage. The following section presents more details of the suggested method.

2. Multiview PMP calibration

Typical PMP calibration methods focus on calculating *only* height information from phase shifts. In contrast, we extend the traditional formulation from phase to height in order to devise a novel PMP model that yields 3D global coordinates. Using our novel calibration target, we can calibrate coefficients of our PMP model from a single static scene without moving and rotating the target for both multi-view and multi-projector configurations. The proposed PMP model is a total calibration process of a system that consists of a camera and a projector. In particular, no separate calibration of the projector is required.

* Corresponding author.
E-mail address: minhkim@vclab.kaist.ac.kr (M.H. Kim).

http://dx.doi.org/10.1016/j.optlaseng.2017.06.012
Received 25 April 2017; Received in revised form 8 June 2017; Accepted 10 June 2017
0143-8166/

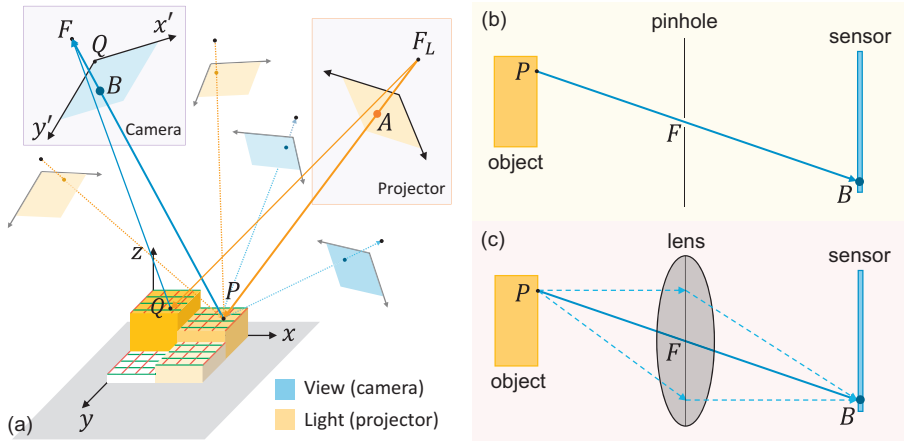

Fig. 1. (a) Schematic diagram of our multi-sensor PMP setup. Images (b) and (c) compare a theoretical pinhole model for a camera and a projector and a lens model for both real devices. Refer to Section 4.2 for detailed discussions on the differences of these models.

2.1. Phase to height

Our calibration starts to determine the geometric relationship from phase to height by inheriting the PMP parameterization [1]. Suppose we have a pair of a pinhole camera and a pinhole projector in a system (each center of projection is represented as F and F_L) as shown in Fig. 1(a). Refer to Section 4.2 for more detailed discussion between the pinhole and the lens camera model.

When a pixel A of phase ϕ from the projector illuminates an object surface, the camera captures the phase ϕ at a point P as a pixel B in the camera frame. Depending on the height z_P at the point P, a different phase is captured at the pixel B. By formulating this relationship, we can derive a height z_P at a pixel (i, j) from a given phase ϕ, following Du et al. [1]:

$$D(\phi, i, j) = \frac{C_0 + C_1\phi + (C_2 + C_3\phi)i + (C_4 + C_5\phi)j}{D_0 + D_1\phi + (D_2 + D_3\phi)i + (D_4 + D_5\phi)j}, \tag{1}$$

where $C_0, \ldots, C_5$ and $D_0, \ldots, D_5$ are twelve unknown coefficients that describe the geometric relationship and properties of the camera and the projector. We can determine these coefficients by solving an objective function S_z with a set of images with M pixels captured with different phases of a height-known target object:

$$S_z = \sum_{k=1}^{M} \left[C(\phi_k, i_k, j_k)/D(\phi_k, i_k, j_k) - z_k\right]^2. \tag{2}$$

We solve the objective function S_z by using linear approximation through partial derivatives. Note that in this formulation (Eq. (1)), the height information is stored per pixel in the camera frame. Therefore, x and y coordinates in the global frame are still unknown, unless calibrating the parameters of the camera using the Zhang method [7] or an additional calibration with moving the scene.

2.2. Phase to 3D global coordinates

As shown in Fig. 1(a), a point on an object can be presented in both the camera coordinates (x', y', z') and the global coordinates (x, y, z), respectively. Since our objective is to measure global coordinates (x_P, y_P, z_P) of point P, we next describe how to determine xy-plane global coordinates in addition to z_P, which we can derive from Eq. (1). Suppose a point P on an object, a pixel point B on the screen and the center of projection (COP) F of the camera are co-linear. We can derive a simple proportional expression of three points' x and z coordinates in the global frame: $x_F - x_B : x_F - x_P = z_F - z_B : z_F - z_P$. We can then rewrite this expression to determine x_P:

$$x_P = x_F - (x_F - x_B)(z_F - z_P)/(z_F - z_B). \tag{3}$$

In order to obtain global coordinates from captured images, we can substitute the global coordinates x_B and z_B of the pixel point B with corresponding screen coordinates x'_B and z'_B. The transformation between global and screen coordinates is formulated as general Euler rotations and translation as follows:

$$\begin{bmatrix} x_B \\ y_B \\ z_B \end{bmatrix} = \begin{bmatrix} x_Q \\ y_Q \\ z_Q \end{bmatrix} + R_z(\gamma)R_y(\beta)R_x(\alpha)\begin{bmatrix} x'_B \\ y'_B \\ z'_B \end{bmatrix}, \tag{4}$$

where α, β and γ are rotating angles for each axis from the camera to the global coordinates. Note that z'_B is set to zero as B stands on the image plane. After substituting x_B and z_B in Eq. (3) using Eq. (4), we can rewrite the expression for x_P:

$$\begin{aligned} x_P = {} & \frac{(z_P - z_F)(x_Q + \cos\beta\cos\gamma \cdot x'_B)}{z_Q - \sin\beta \cdot x'_B + \sin\alpha\cos\beta \cdot y'_B - z_F} \\ & + \frac{(z_P - z_F)(-\cos\alpha\sin\gamma + \sin\alpha\sin\beta\cos\gamma)y'_B}{z_Q - \sin\beta \cdot x'_B + \sin\alpha\cos\beta \cdot y'_B - z_F} \\ & + \frac{(z_Q - \sin\beta \cdot x'_B + \sin\alpha\cos\beta \cdot y'_B - z_P)x_F}{z_Q - \sin\beta \cdot x'_B + \sin\alpha\cos\beta \cdot y'_B - z_F}. \end{aligned} \tag{5}$$

In this equation, except the screen coordinates (x'_B, y'_B) of the pixel point B, and the object height (z_P), the rest of the variables remain constant: the global coordinates of COP (x_F, y_F, z_F), the global coordinates of the origin of the camera plane (x_Q, z_Q), and the XYZ rotation angles of the camera frame (α, β and γ) as long as the geometric configuration of system elements remains unchanged. We hence can substitute these variables as constants: $-z_F x_Q + z_Q x_F \to E_1$, $-\cos\beta\cos\gamma \cdot z_F - \sin\beta \cdot x_F \to E_2$, $(\cos\alpha\sin\gamma - \sin\alpha\sin\beta\cos\gamma) \cdot z_F + \sin\alpha\cos\beta \cdot x_F \to E_3$, $x_Q - x_F \to E_4$, $\cos\beta\cos\gamma \to E_5$, $-\cos\alpha\sin\gamma + \sin\alpha\sin\beta\cos\gamma \to E_6$, $z_Q - z_F \to E_7$, $-\sin\beta \to E_8$ and $\sin\alpha\cos\beta \to E_9$. We can write Eq. (5) as follow:

$$x_P = \frac{E_1 + E_2 x'_B + E_3 y'_B + (E_4 + E_5 x'_B + E_6 y'_B)z_P}{(E_7 + E_8 x'_B + E_9 y'_B)}. \tag{6}$$

Our goal is to estimate the global coordinates of the object from captured phases. Therefore, we need to formulate Eq. (6) as an expression for (ϕ, i, j). Note that the screen coordinates (x'_B, y'_B) in Eq. (6) are the same as the pixel position (i, j) in Eq. (1). We also can substitute z_P with Eq. (1) to rewrite Eq. (6) as follows:

$$x_P = \frac{G(\phi, i, j)}{H(\phi, i, j)} \tag{7}$$

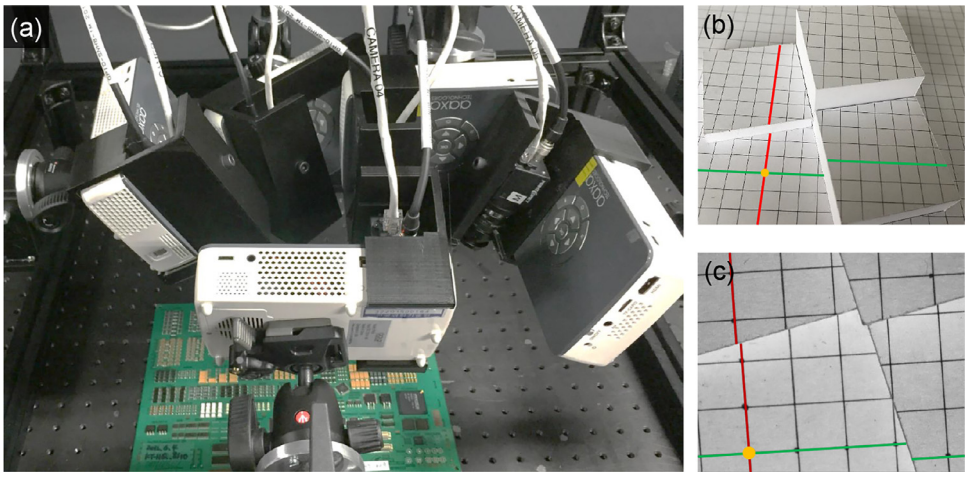

Fig. 2. (a) presents our experimental setup. (b) our calibration target. (c) shows the captured image of the target from a view.

$$G(\phi,i,j) = G_0 + G_1\phi + G_2 i + G_3 j + G_4\phi i + G_5\phi j + G_6 i^2 + G_7 j^2 + G_8 ij + G_9\phi i^2 + G_{10}\phi j^2 + G_{11}\phi ij,$$
$$H(\phi,i,j) = H_0 + H_1\phi + H_2 i + H_3 j + H_4\phi i + H_5\phi j + H_6 i^2 + H_7 j^2 + H_8 ij + H_9\phi i^2 + H_{10}\phi j^2 + H_{11}\phi ij,$$

where $G_0,\dots,G_{11}$ and $H_0,\dots,H_{11}$ are the constant coefficients on static PMP setup. These unknown coefficients can be estimated through our PMP calibration by minimizing the following objective function S_x using x-known N_x pixels:

$$S_x = \sum_{k=1}^{N_x} \left[G(\phi_k,i_k,j_k)/H(\phi_k,i_k,j_k) - x_k\right]^2. \quad (8)$$

In the same manner, the phase-to-y mapping model and the objective function for y_P can be derived. This allows us to determine three-dimensional global coordinates of a point P from the captured phase ϕ and pixel position (i, j) of P, without additional calibration process.

2.3. Calibration target design

While the Du and Wang calibration method [1] determines 12 coefficients in Eq. (1) using standard gauge blocks, our calibration needs to determine 24 coefficients for both the x and y axes of the global coordinate system, respectively, in addition to 12 coefficients for height. To do so, we design a novel calibration target that has multiple gauge blocks of different heights with uniform x, y grid lines on the top of blocks. Different from existing calibration methods with multiple gauge blocks [1,3,4], we map the grid lines to x-known and y-known pixels for determining unknown coefficients in Eq. (7). In our experiment, the heights of the used blocks are 0 (ground), 5, 10, and 20 mm, and the interval between grid lines is 5 mm. The object in Fig. 1(a) shows a schematic overview of calibration target. And Fig. 2(b) and (c) show our prototype calibration target and a captured image from one view. The red line of the gauge blocks is mapped to the x axis in the global frame, while the green line is mapped to the y axis. The yellow dot highlights the cross section of these two axes; i.e., the yellow point is mapped to the origin of the global coordinate system.

2.4. Phase extraction

We use four-phase intervals of $\pi/2$ for each frequency to detect phase ϕ at pixel (x, y), as with typical PMP methods [4,17]: $I_i(x,y) = I_b(x,y) + I_a(x,y)\sin\{2\pi\cdot f(x) + \phi(x,y) + (i-1)\frac{\pi}{2}\}$, where I_b is the base intensity of the sinusoidal pattern at a pixel (x, y), I_a is the amplitude of the intensity modulation, ϕ is the phase value in the sinusoidal pattern, and $i \in [1, 4]$ indicates each phase shift. Since we have four equations (with four phase-shifts) with three unknowns of I_a, I_b and ϕ at a pixel (x, y), we can solve an overdetermined system using $\phi(x,y) = \tan^{-1}\left[\{I_1(x,y) - I_3(x,y)\}/\{I_2(x,y) - I_4(x,y)\}\right]$. The calculated phase value from $-\pi$ to π is transformed to the range of zero to 2π. We illuminate four different frequencies in our experiments to utilize a temporal unwrapping method [18].

3. Results

To validate our proposed method, we implemented it as a prototype, as shown in Fig. 2(a). Our prototype includes five pairs of a camera (PointGrey Blackfly) and a DLP projector (AXAA P450) on a supporting structure. Fig. 2(b) and (c) show our calibration target and an acquired image from one view. First, we calibrated our system with the proposed calibration method and our target. We then reconstruct several objects a 5.3 mm-height cube with 5.0 mm-grid, a ceramic object (Chinese doll) and a chip of electronic circuit board to evaluate the measurement, quantitatively and qualitatively.

3.1. Quantitative evaluation

To validate the measurement accuracy and precision of our method, we scanned 5.3 mm-height cube with 5.0 mm intervals grids, using 12 valid camera-projector PMP combinations in the system. (Since we use 5 camera-project pairs, technically 25 combinations of the cameras and projectors are available. However, considering ray directions and occlusions, we end up with 12 valid combinations. It will be discussed on Section 4.)

We measured the height of 20 points (P_1 to P_{20} in Fig. 3) and length of 29 edges (L_1 to L_{29} in Fig. 3) on the cube, which are visible from both cameras, yielding three-dimensional global coordinates. The right plots show the average measured height of 20 points and the length of 29 lines from 12 valid combinations. It shows that our measurements present a strong agreement with the reference height and length. The average height error of 20 points from 12 valid PMP combinations is approximately 70.5 μm and the maximum error of the entire height measurements is 219.3 μm. And the average standard deviation for height measurement of 20 points from 12 valid PMPs is 82.0 μm. The average length error of 29 lines is approximately 26.5 μm and the maximum error is 82.4 μm. And the average standard deviation for length measurement of 29 lines from 12 valid PMPs is 31.1 μm. The low average error from this experiment supports that our proposed method is very accurate compared with reference. And the low average standard deviation from 12 valid PMPs also support that our method are highly precise, i.e., all these measured results from 12 valid PMPs are very accurate. Also, measuring accurate Euclidean length means that our proposed method

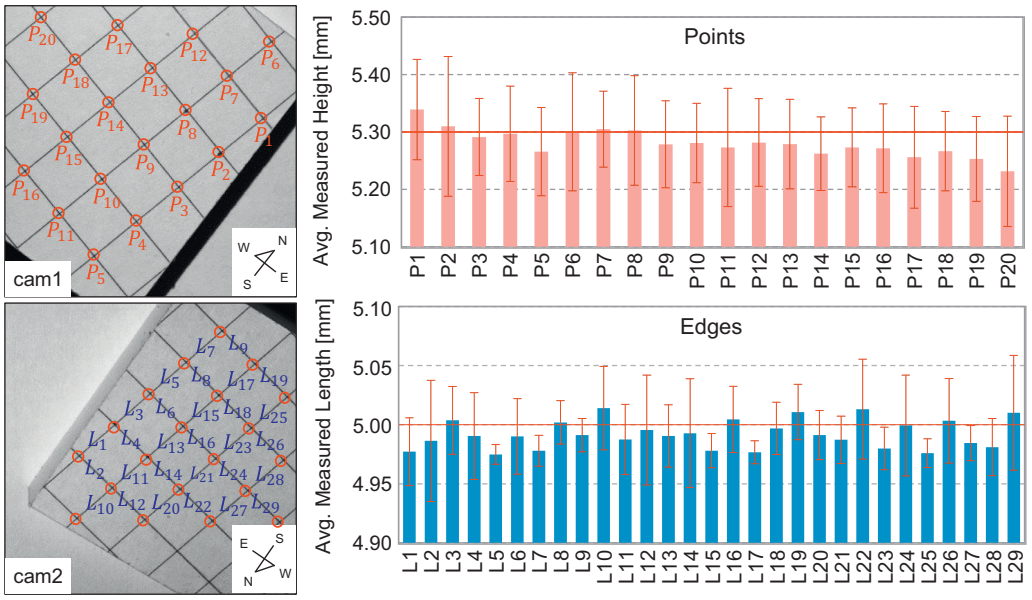

Fig. 3. Two view examples of a 5.3 mm-height cube with 5 mm grids. We measure the height of 20 points and the length of 29 edges visible from five different views (total 12 valid PMPs) and compare the measurements with the reference height (5.3 mm) and length (5.0 mm). Right plots show the results.

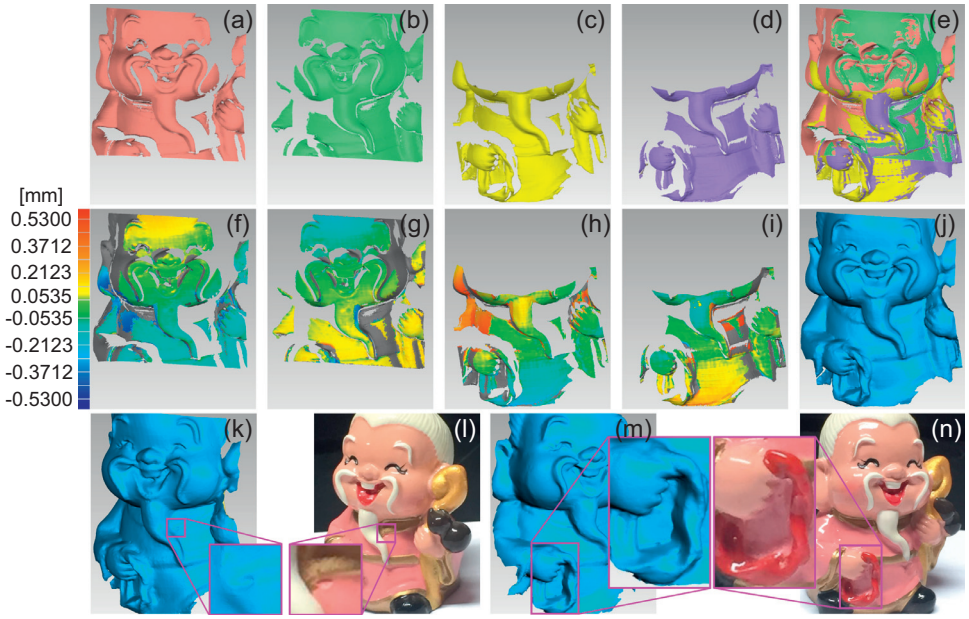

Fig. 4. (a) – (d) Show individual scans from each PMP, and (e) shows an overlapped geometry. (f) – (i) present Euclidean distances of faces at each PMP from the averaged positions of overlapping regions of three different PMPs. Average distance is 102.0 μm and standard deviation is 105.1 μm. (j) exhibits a reconstructed geometry. (k) – (n) show our results with closeups.

estimates the accurate *x, y* and height coordinates in the global space. While the proposed method can provide high accuracy in general, sub-optimal results can be obtained when the angle difference between the projector's and the camera's horizontal axis is not sufficient for solving Eq. (8). Refer to Section 4.1 for more details.

3.2. Qualitative evaluation

To validate the capability and quality of our multiview PMP approach, we scanned a ceramic object (Chinese doll), as shown in Fig. 4. Images (a) to (d) show four individual geometries measured by each PMP from different combinations. Each PMP reveals different sides of the object geometry. Image (e) is an integrated geometry by merely merging them. Since our multiview PMP yields 3D geometries in the global coordinates, we can merge them without introducing any transformation among them. In the second row, Images (f) to (i) present Euclidean distances (*quantitative error*) of faces from each PMP from the averaged positions of overlapping regions from other PMP combinations. Image (j) exhibits a combined geometry model reconstructed via iterative closest points. In the last row, we show results with close-ups. Our multiview PMP method allows us to capture very fine geometry in detail even on specular surfaces, e.g., a concave-shaped surface, as shown in Images (k) – (n).

Fig. 5 exhibits 3D inspection results of a chip (a). In particular, the legs of the chip are thin and specular and thus high-quality 3D scanning is challenging due to specularity and inter-reflection. Image (b) shows a single-view PMP result. Image (c) presents our multi-view PMP result. Multiview PMP allows us to avoid specular reflections at the mirror reflection angle. Since our method enables highly precise alignment of each PMP measurement, our result exhibits more accurate geometry of specular solder joints around legs.

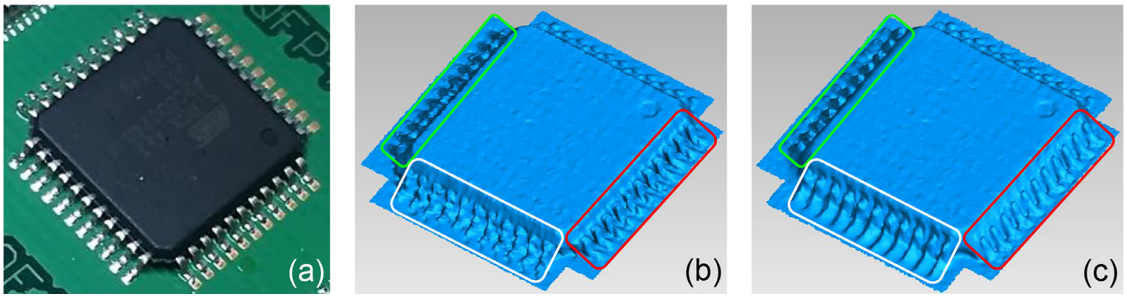

Fig. 5. (a) A chip with specular parts. (b) a single PMP result. Geometry of legs and solder joints cannot be exactly captured due to specularity and inter-reflection. (c) our multiple PMPs result. We can take advantages of multiview PMP to avoid specularity, since our method allows for accurate alignment of multiple PMPs without additional calibration process. The green, white and red rectangles compare measurements between the single and the multiview PMPs. The three regions are measured from three different views in our multiview PMP setup. (For interpretation of the references to colour in this figure legend, the reader is referred to the web version of this article.)

4. Discussion and conclusion

4.1. View combinations

Our multiview PMP allows us to utilize various combinations of cameras and projectors for measuring 3D global geometry. However, owing to the PMP characteristics, not all combinations cannot be used. For instance, when the optical axis of the camera is the same as that of the projector, the PMP formulation becomes invalid. When the frame axes of the camera and the projector are parallel, the formulation also becomes invalid. In our current setup that consists of five cameras and projectors, we found 12 valid combinations among 25. Note that, in these 12 selected combinations, there are suboptimal results from a certain combinations of a camera and a project, where the horizontal axes of the camera and the projector are significantly similar. We found that when there is a large angle difference along the horizontal axis, the accuracy of our measurement increases. The number of valid combinations could be increased by adjusting the orientations and positions of the system setup.

4.2. Real camera and projector

While we assumed the pinhole camera in Section 2, the real camera has a lens rather than a pinhole. If there is no lens distortion, our model can be applied to the real camera in the same manner. Because, in the lens camera, a point P on an object, a pixel point B on the sensor and the COP F of the camera are still co-linear, like a pinhole model (bold blue line in Fig. 1(b) and (c)). In case a lens introduce severe lens distortion in a real camera, we can correct it by using Huang et al. [3]. Our method includes the lens distortion step to the phase to height conversion model (Eq. (1)) following Du and Wang [1]. In addition, inter-reflection between surfaces could be removed following [19]. It remains as our future work.

4.3. Conclusion

We have presented a novel multiview integrated PMP calibration method that yields highly accurate 3D geometry in three-dimensional global coordinates. Our calibration model can directly convert the phase on pixel (i, j) to (x, y, z) global coordinates for any system that consists of cameras and projectors, with no additional calibration process including projector calibration. It enables to integrate several PMP measurements directly. And our new calibration target remains static while calibrating the system setup, avoiding mechanical errors. In addition, our calibration is free from any physical constraints in the setup. Our results validate the accuracy and precision of our method and system. And it also shows the usefulness of the proposed integrated multiview PMP calibration approach.

Acknowledgements

Min H. Kim gratefully acknowledges Korea NRF grants (2016R1A2B2013031, 2013M3A6A6073718) and additional support by Koh Young Technology, Samsung Electronics (SRFC-IT1402-02), Cross-Ministry Giga KOREA Project (GK17P0200), Korea Creative Content Agency (KOCA) in Ministry of Culture, Sports and Tourism (MCST), and an ICT R&D program of MSIP/IITP of Korea (R7116-16-1035).

References

[1] Du H, Wang Z. Three-dimensional shape measurement with an arbitrarily arranged fringe projection profilometry system. Opt Lett 2007;32(16):2438–40.
[2] Zhang Z, Ma H, Zhang S, Guo T, Towers CE, Towers DP. Simple calibration of a phase-based 3D imaging system based on uneven fringe projection. Opt Lett 2011;36(5):627–9.
[3] Huang L, Chua PSK, Asundi A. Least-squares calibration method for fringe projection profilometry considering camera lens distortion. Appl Opt 2010;49(9):1539–48.
[4] Fu Y, Wang Y, Wang W, Wu J. Least-squares calibration method for fringe projection profilometry with some practical considerations. Optik Int J Light Electron Opt 2013;124(19):4041–5.
[5] Xiao S, Tao W, Yan H, Zhao H. A new geometrical model and mathematical method for three-dimensional surface reconstruction based on phase-shifting structured light technique. In: Proc. SPIE, 9276; 2014. p. 92761Z–92761Z–10.
[6] Albers O, Poesch A, Reithmeier E. Flexible calibration and measurement strategy for a multi-sensor fringe projection unit. Opt Express 2015;23(23):29592.
[7] Zhang Z. A flexible new technique for camera calibration. IEEE Trans Pattern Anal Mach Intel 2000;22(11):1330–4.
[8] Zhang Z, Huang S, Meng S, Gao F, Jiang X. A simple, flexible and automatic 3D calibration method for a phase calculation-based fringe projection imaging system. Opt Express 2013;21(10):12218–27.
[9] Huang Z, Xi J, Yu Y, Guo Q, Song L. Improved geometrical model of fringe projection profilometry. Opt Express 2014;22(26):32220.
[10] Xiao Y, Cao Y, Wu Y. Improved algorithm for phase-to-height mapping in phase measuring profilometry. Appl Opt 2012;51(8):1149–55.
[11] Vo M, Wang Z, Pan B, Pan T. Hyper-accurate flexible calibration technique for fringe-projection-based three-dimensional imaging. Opt Express 2012;20(15):16926–41.
[12] Meng S, Ma H, Zhang Z, Guo T, Zhang S, Hu X. Complete calibration of a phase-based 3D imaging system based on fringe projection technique. In: Int. conf. optical instruments and technology: optoelectronic imaging and processing technology, 8200; 2011. p. 82000L.
[13] Nam G, Lee JH, Wu H, Gutierrez D, Kim MH. Simultaneous acquisition of microscale reflectance and normals. ACM Trans Graph 2016;35(6).
[14] Liu H, Su WH, Reichard K, Yin S. Calibration-based phase-shifting projected fringe profilometry for accurate absolute 3D surface profile measurement. Opt Commun 2003;216:65–80.
[15] Zhu F, Shi H, Bai P, He X. Three-dimensional shape measurement and calibration for fringe projection by considering unequal height of the projector and the camera. Appl Opt 2011;50(11):1575–83.
[16] Villa J, Araiza M, Alaniz D, Ivanov R, Ortiz M. Transformation of phase to (x,y,z)-coordinates for the calibration of a fringe projection profilometer. Opt Lasers Eng 2012;50(2):256–61.
[17] Gdeisat M, Qudeisat M, AlSa'd M, Burton D, Lilley F, Ammous MM. Simple and accurate empirical absolute volume calibration of a multi-sensor fringe projection system. Opt Laser Eng 2016;80:32–44.
[18] Tian J, Peng X, Zhao X. A generalized temporal phase unwrapping algorithm for three-dimensional profilometry. Opt Lasers Eng 2008;46:336–42.
[19] Nam G, Kim MH. Multispectral photometric stereo for acquiring high-fidelity surface normals. IEEE Comput Graph Appl 2014;34(6):57–68.